LA-UR-15-29086
Approved for public release; distribution is unlimited.

Title: Response of Cs2LiYCl6:Ce (CLYC) to High Energy Protons

Author(s): Coupland, Daniel David Schechtman
Stonehill, Laura Catherine
Goett, John Jerome III

Intended for: 2015 IEEE Nuclear Science Symposium and Medical Imaging Conference, 2015-11-02 (San Diego, California, United States)

Issued: 2015-11-23

Response of Cs_2LiYCl_6:Ce (CLYC) to High Energy Protons

Coupland, Daniel D. S., Stonehill, Laura C., and Goett, John J. III

***Abstract*—Cs_2LiYCl_6:Ce (CLYC) is a promising new inorganic scintillator for gamma and neutron detection. As a gamma-ray detector, it exhibits bright light output and better resolution and proportionality of response than traditional gamma-ray scintillators such as NaI. It is also highly sensitive to thermal neutrons through capture on ^{6}Li, and recent experiments have demonstrated sensitivity to fast neutrons through interactions with ^{35}Cl. The response of CLYC to other forms of radiation has not been reported. We have performed the first measurements of the response of CLYC to several-hundred MeV protons. We have collected digitized waveforms from proton events, and compare to those produced by gammas and thermal neutrons. Finally we discuss the potential for pulse shape discrimination between them.**

I. Introduction

ELPASOLITES are a promising new family of inorganic scintillators for duel-mode gamma and neutron detection. The most studied member of the elpasolites is $Cs_2LiYCl_6:Ce^{3+}$ (CLYC). It emits at a peak wavelength of 373 nm (well-matched to many commercial photomultiplier tubes), has a density of 3.31 g/cm3, and produces a bright light output of 20,000 photons per MeV electron equivalent. For gamma spectroscopy it provides an energy resolution of 4% at 662 keV, better than commonly-used NaI crystals[1]. CLYC also provides thermal neutron sensitivity by means of the ^{6}Li(n$_{th}$,α)T reaction and fast neutron sensitivity by means of both the ^{6}Li(n,α)T and ^{35}Cl(n,p)^{35}S reactions[2]. Differences in scintillation decay times allow gammas to be distinguished from neutrons using pulse shape discrimination (PSD). The ability to detect and distinguish between gamma and neutron radiation in a single material is attractive for applications where size and complexity are limiting factors, such as hand-held radiation detection.

While the response of CLYC to gammas and neutrons has been extensively studied, the response to other forms of radiation is also of interest. The response to interactions with different ionization density can inform models of the scintillation mechanism. In addition, charged particle radiation is a source of background for space-based radiation detection, which is another application where reduction in detector size and complexity is beneficial. We have measured for the first time the response of CLYC to protons with energies of hundreds of MeV.

D. D. S. Coupland and L. C. Stonehill are with the Space Science and Applications Group of Los Alamos National Laboratory, Los Alamos, NM, 87545 USA e-mail: dcoupland@lanl.gov

J. J. Goett, III is with the Neutron Science and Technology Group of Los Alamos National Laboratory, Los Alamos, NM, 87545 USA

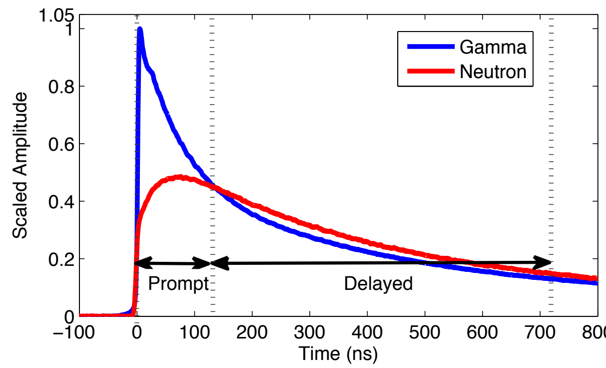

Fig. 1. Waveforms produced by neutrons and gamma interactions in CLYC, indicating optimal prompt and delayed integration windows.

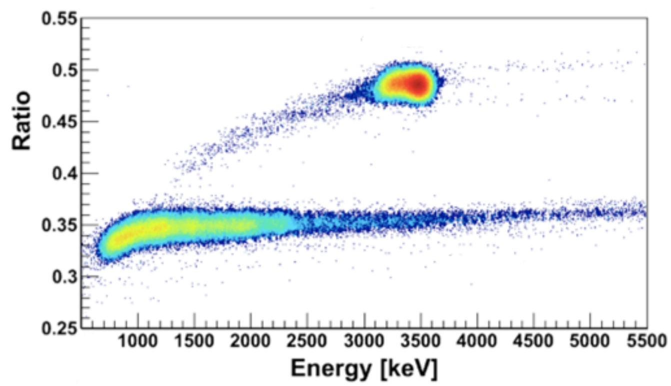

Fig. 2. Example gamma and neutron PSD in CLYC. In this figure, neutrons are clustered between 3000 and 3500 keV with a PSD ratio of 0.5, while gammas contribute to a energy continuum with a PSD ratio of 0.35.

II. Pulse Shape Discrimination

Several scintillation mechanisms with different time constants contribute to the light output from CLYC[3]. The contribution from the different mechanisms changes depending on the incident particle, so that different incident particles produce light with different time profiles, as shown in Figure 1. By integrating over appropriate prompt (P) and delayed (D) windows, we form the pulse shape discrimination (PSD) ratio R:

$$R = \frac{D}{P + D} \tag{1}$$

which discriminates between particles types. An example CLYC PSD histogram is shown in Figure 2. The pulse shape of fast protons and whether fast protons can be distinguished from other particles types has not been reported previously.

Fig. 3. Beamline exit window, viewed from the location of the CLYC crystal.

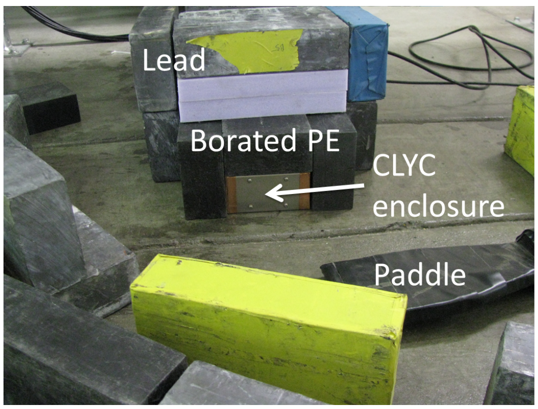

Fig. 4. Partially deconstructed shield hut surrounding the CLYC crystal. The aluminum enclosure at the center housed and protected the smaller CLYC crystal, and the plastic scintillator paddle was placed inside the shield bricks, next to the CLYC enclosure.

III. Experimental Setup

Protons were produced at the Los Alamos Neutron Science Center (LANSCE), accelerated to an energy of 800 MeV, and delivered to the Proton Radiography (pRad) experimental area[4]. The beam was delivered in bursts of more than 10^8 protons in an interval of 5 ns. Several bursts separated by tens of μs were delivered in a given burst train. Because we were interested in the interaction of single particles, we could not place a CLYC crystal directly in the beamline. Instead, we placed a 1 cm^3 CLYC crystal 10 m away from a thin beam window, shown in Figure 3, and 30° off the beamline to detect scattered protons.

We surrounded the CLYC crystal with 2 inches each of lead and borated polyethylene bricks to reduce the background from gammas and neutrons, respectively. A plastic scintillator paddle in front of the crystal indicated the arrival of protons. Neither the crystal nor the shielding were thick enough to stop 800 MeV protons. Figure 4 shows the shielding around the CLYC, partially deconstructed to expose the shield layers.

A Hamamatsu R11265-100 PMT collected the light from the CLYC crystal. An Agilent U1065A Acqiris DC282 waveform digitizer sampled the waveforms every 500 ps.

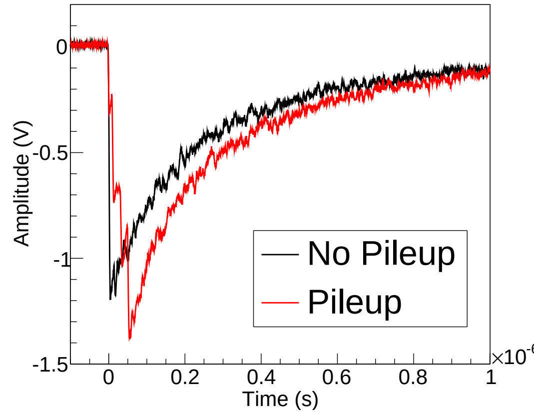

Fig. 5. A comparison of waveforms with and without pileup.

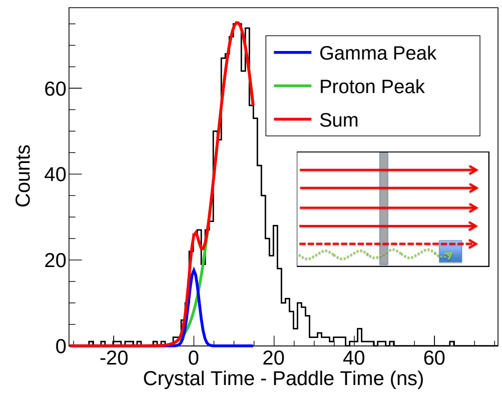

Fig. 6. Time spectrum of all events, including pileup. The initial gamma peak is offset to time 0. Inset: a schematic of many protons (red) interacting with the plastic scintillator (gray) while a single proton or gamma (green) interacts with the CLYC.

IV. Analysis

We first selected interesting events by a coincidence between the plastic scintillator and the CLYC crystal. Even so far from the scattering location, many CLYC waveforms exhibited pileup. We visually inspected waveforms to select events without pileup, most of which occurred during initial beam tuning when the proton beam was not well focused into the pRad dome. Representative waveforms with and without pileup are given in Figure 5.

The plastic scintillator was much larger than the 1 cm^3 CLYC and so experienced a large number of proton interactions in each event, even when the CLYC experienced only a single gamma or proton interaction. This is diagrammed in the inset of Figure 6. While protons scattered off the beamline exit window at many energies, so many interacted with the plastic scintillator in each event that the first proton to reach the plastic in each event was at the upper end of the energy distribution. The start of the signal in the plastic was thus an approximately constant time after the beam pulse, while the interaction in the CLYC may be earlier if it was a gamma, or later if it was a slower proton. Subtracting the time in the plastic from the time in the CLYC gives the

TABLE I
INTEGRATION WINDOWS USED TO CONSTRUCT PSD PLOTS.

Window	Start	End
Prompt (n/γ)	0 ns	120 ns
Delayed (n/γ)	120 ns	800 ns
Prompt (γ/p)	0 ns	35 ns
Delayed (γ/p)	35 ns	400 ns
Energy	0 ns	10 μs

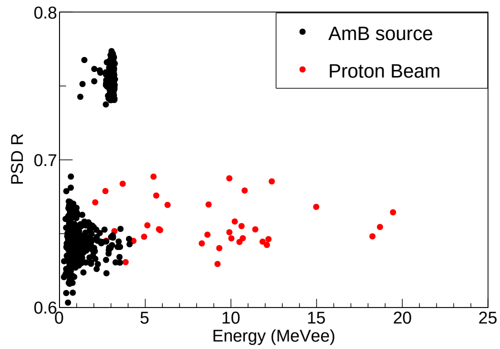

Fig. 7. PSD from proton events compared to gamma and neutron events from an AmB source. Thermal neutrons capture from the AmB source are grouped near 3 MeV electron equivalent and a PSD ratio of 0.75, while gammas and fast protons form a continuum in energy near a PSD ratio of 0.65.

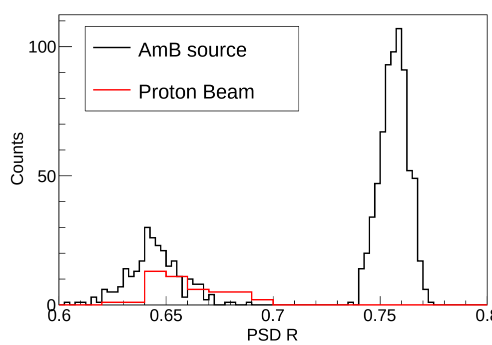

Fig. 8. Projected PSD from Figure 7.

spectrum in Figure 6. Pileup events were included in this figure to improve statistics. A smaller Gaussian peak, offset to time zero, indicates the arrival of prompt gammas in the CLYC, while later events are protons. Removing events in the gamma peak, the remaining 36 events without CLYC pileup are protons with energies between 150 and 700 MeV as indicated by TOF and simulated energy loss in the shielding.

V. Results

In Figure 7, we plot the PSD ratio R versus deposited from the identified proton events compared to gamma and neutron events from an AmB source. In this figure, we use integration windows appropriate for neutron and gamma discrimination, labeled γ/p in Table I, and in Figure 8 we project the histogram onto the PSD axis. The pulse shape ratio from proton events does not show a trend with deposited energy. It is similar to that of gammas but there is a systematic shift toward larger

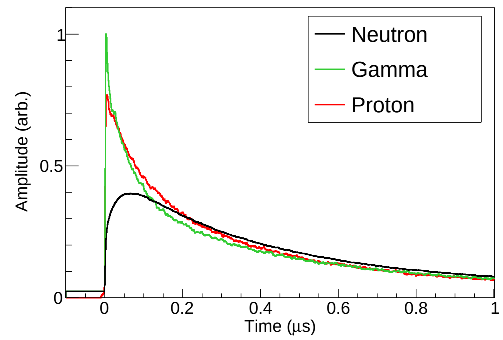

Fig. 9. Average waveforms from events shown in Figures 7 and 8.

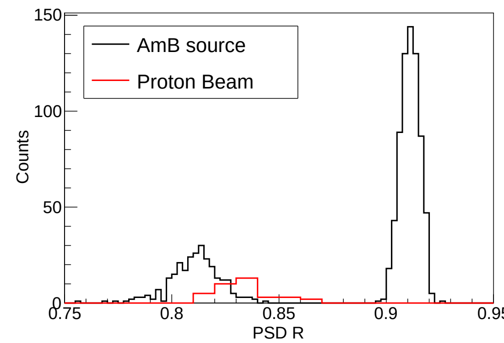

Fig. 10. Projected PSD using the shorter windows from Table I.

values.

To explore the possibility of PSD between γ and proton events more fully, we construct average waveforms from the neutron, gamma, and proton events separately (Figure 9). The proton average waveform is very similar but not identical to the gamma waveform. The times when the average waveforms cross suggest more appropriate integration times for proton PSD, marked γ/p in Table I. Constructing the PSD R with these values (10) demonstrates improved discrimination between proton and gamma events on average, although the distributions overlap. The thermal neutron and gamma peaks are still well-separated with these windows.

VI. Conclusions

Fast protons interactions that do not stop in a CLYC crystal give rise to pulse shapes very similar to gamma interactions. Since pulse shape differences generally arise from the ionization density of the interaction and these protons are nearly minimum ionizing, that result is to be expected. However, there are slight differences between gamma and fast proton waveforms that can be exploited to distinguish between them on average if not event-by-event.

Acknowledgment

We gratefully acknowledge the support of the pRad team, particularly Matthew Murray, as they accommodated our needs during their own experimental operations.

REFERENCES

[1] J. Glodo, R. Hawrami, and K. Shah, "Development of cs2liycl6 scintillator," *Journal of Crystal Growth*, vol. 379, no. 0, pp. 73 – 78, 2013, compound Semiconductors and Scintillators for Radiation Detection Applications: A Special Tribute to the Research of Michael Schieber. [Online]. Available:

[2] N. D'Olympia, P. Chowdhury, C. J. Lister, J. Glodo, R. Hawrami, K. Shah, and U. Shirwadkar, "Pulse-shape analysis of clyc for thermal neutrons, fast neutrons, and gamma-rays," *NUCLEAR INSTRUMENTS & METHODS IN PHYSICS RESEARCH SECTION A-ACCELERATORS SPECTROMETERS DETECTORS AND ASSOCIATED EQUIPMENT*, vol. 714, pp. 121–127, JUN 21 2013.

[3] B. S. Budden, L. C. Stonehill, J. R. Terry, A. V. Klimenko, and J. O. Perry, "Characterization and investigation of the thermal dependence of cs2liycl6 : Ce3+ (clyc) waveforms," *IEEE TRANSACTIONS ON NUCLEAR SCIENCE*, vol. 60, no. 2, 1, pp. 946–951, APR 2013, symposium on Radiation Measurements and Applications (SORMA), Oakland, CA, MAY 14-17, 2012.

[4] N. King, E. Ables, K. Adams, K. Alrick, J. Amann, S. Balzar, P. B. Jr, M. Crow, S. Cushing, J. Eddleman, T. Fife, P. Flores, D. Fujino, R. Gallegos, N. Gray, E. Hartouni, G. Hogan, V. Holmes, S. Jaramillo, J. Knudsson, R. London, R. Lopez, T. McDonald, J. McClelland, F. Merrill, K. Morley, C. Morris, F. Naivar, E. Parker, H. Park, P. Pazuchanics, C. Pillai, C. Riedel, J. Sarracino, F. S. Jr, H. Stacy, B. Takala, R. Thompson, H. Tucker, G. Yates, H.-J. Ziock, and J. Zumbro, "An 800-mev proton radiography facility for dynamic experiments," *Nuclear Instruments and Methods in Physics Research Section A: Accelerators, Spectrometers, Detectors and Associated Equipment*, vol. 424, no. 1, pp. 84 – 91, 1999.